Converter-level reliability of wind turbine with low sample rate mission profile

Zhou, Dao; Blaabjerg, Frede

Published in:
I E E E Transactions on Industry Applications

DOI (link to publication from Publisher):
10.1109/TIA.2020.2977301

Publication date:
2020

Document Version
Accepted author manuscript, peer reviewed version

This article has been accepted for publication in a future issue of this journal, but has not been fully edited. Content may change prior to final publication. Citation information: DOI 10.1109/TIA.2020.2977301, IEEE Transactions on Industry Applications

Converter-level Reliability of Wind Turbine with Low Sample Rate Mission Profile

Dao Zhou, *Senior Member, IEEE*, and Frede Blaabjerg, *Fellow, IEEE*

Department of Energy Technology
Aalborg University, Aalborg, Denmark
zda@et.aau.dk; fbl@et.aau.dk

***Abstract* - The thermal dynamics of power semiconductors and power capacitors are closely related to the reliability and affect the cost of power electronic converter. However, the component loading in a wind turbine system is disturbed by many factors of the power converter, which presents various time-constants from micro-seconds to hours. To determine the system availability in such system is a challenge and need detailed analysis. In the case of a mission profile with 1-hour sample rate, a simplified circuit model, loss model, and thermal model of the active power switches and passive capacitors are needed and described. According to the long-term electro-thermal profile, the percentile lifetime of a single component can be predicted. The Weibull function based time-to-failure distribution can then be used to link from component-level to converter-level reliability. From analysis of a 2 MW wind turbine system, it can be seen that the DC-link capacitor bank dominates the converter-level reliability.**

I. INTRODUCTION

Power electronics are being widely used in many energy conversion systems like renewable energy, motor drives, and power transmission. The reliability and cost requirements for power electronic systems are getting more critical [1], [2]. Nevertheless, a survey presented in [3] finds that approximately 37% of the total unexpected failures of a 3.5 MW photovoltaic plant are caused by the inverter. Moreover, the cost of inverter failures even reaches 59%, which classifies the power converter as the bottleneck seen from the system-level reliability. A component-level reliability survey has been carried out in [4], and it concludes that the power devices and capacitors are the most fragile components of the power electronic system. Consequently, many research efforts have been devoted to the reliability evaluation of these active and passive components.

The power devices are subjected to a variety of temperature profiles, which cause cyclic thermo-mechanical stress in all the layouts and joints of the modules and finally lead to device failure. Due to the considerably thermal expansion coefficients difference among the module layers, the bond wires, chip solder joints and substrate solder joints suffer most from the thermal stress. As discussed in [5], the lifetime model for the solder joint is based on the time-dependent creep and therefore the cycle period affects the solder joint lifetime. However, the lifetime model for the bond wire is independent on the cycle period, as this model assumes that the immediate plastic deformation leads to fatigue instead of time-dependent creep. Besides, there are two kinds of thermal cycles in the power semiconductors [6], [7]. One is the loading variation based thermal cycles, which are caused by different loading current and ambient temperature with cycle period from seconds to years. The other kind is the fundamental-frequency based thermal cycles ranging from milliseconds to seconds, which are induced by the complementary conduction between the IGBTs and the freewheeling diodes within a fundamental period of the AC current.

In respect to the power capacitor, its thermal performance is complicated and highly affected by the operation conditions, such as the voltage, current, frequency, and temperature. In the application of high power generation, various types of capacitors are selected in the power conversion stage. The aluminum electrolytic capacitors (Al-CAP) are normally used in the DC-side due to its lower cost and higher power density. However, the metalized polypropylene film capacitors (MPF-CAP) are generally applied in the AC-side grid filter because of its ability to withstand higher voltage and longer lifetime. Plenty of literature has studied the electrical stresses of the Al-CAP used in the DC-link with various modulation techniques, converter topologies, and power grid conditions [8]-[13]. On one hand, simulation software is applied to evaluate the harmonic spectrum of the DC-link without any theoretical calculations of the capacitor current [9]. An alternative is to calculate the PWM harmonics of the capacitor by using the time-consuming and complicated double Fourier analysis [10], [11], [13], where the high-order harmonics from a single grid-connected converter is investigated. In addition, the electrical stresses of the DC-link capacitor are the key focuses in these studies, which ignore another important industry concern – the thermal stress and lifetime of the DC-link capacitor. With respect to the AC-side MPF-CAP, lots of studies focusing on the design procedure of the LCL filter and its control methods for the power quality and system stability improvement are done [14], [15]. Nevertheless, few research efforts have been devoted to evaluate the electrical behavior and lifecycle prediction of the film capacitor.

A typical wind power system is illustrated in Fig. 1, and the main disturbances for the thermal behavior of the power

This article has been accepted for publication in a future issue of this journal, but has not been fully edited. Content may change prior to final publication. Citation information: DOI 10.1109/TIA.2020.2977301, IEEE Transactions on Industry Applications

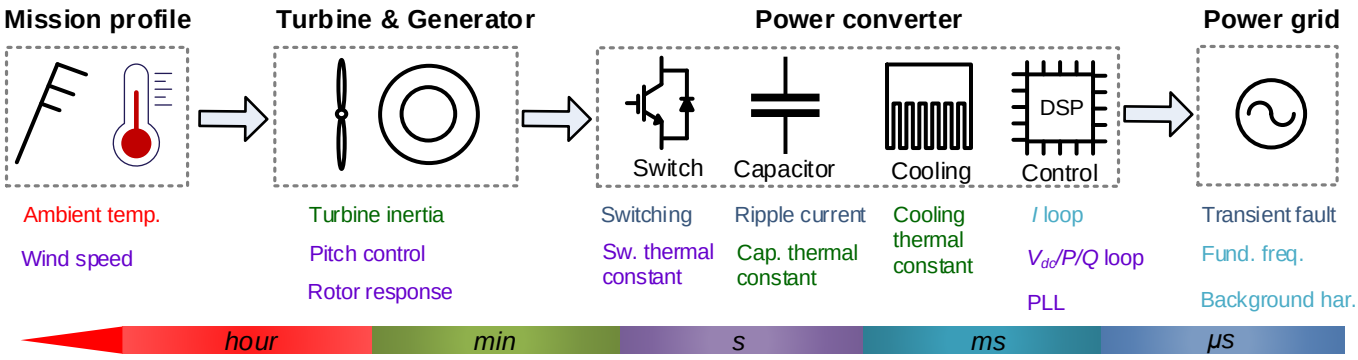

Fig. 1. Timescale of mechanical and electrical components in wind turbine system.

semiconductors and capacitors are summarized according to their dominant response time. It is noted that these thermal disturbances have very different time constants ranging from microseconds (device switching, capacitor ripple current) to hours (ambient temperature changing), making the sampling step of the models in the converter system hard to be decided. The existing models for power electronics seem not good enough to reflect the thermal performance: either very detailed circuit models are applied but restrained to limited timespan and small time-step [16], or only steady-state conditions are assumed with a compromised accuracy of many of the important thermal dynamics [17].

The background of this study is related to a 2 MW Doubly-Fed Induction Generator (DFIG) based wind turbine system, which requires high reliability (i.e., 0.95) within a service life of 20 years. In respect to the whole converter-level reliability evaluation, the prior-art approaches assume that it is dominated by the most fragile component [17], [18]. However, this method neglects the impacts from other components. The motivation of this paper is to predict the reliability of the power converter at the end of service life to identify the bottleneck components and to better size the key components for the next generation product. The novel aspects of the proposed method for reliability evaluation are as follows: 1) propose efficient and simplified models with low sample rate mission profile, and 2) obtain the component-level lifetime distribution considering the parameter variations in the lifetime model, in order to facilitate the converter-level reliability calculation linked by the reliability block diagram.

The rest of the paper is organized as follows: Section II gives an approach to evaluate the component-level reliability of power semiconductors. Section III investigates the annual damage of power capacitors considering the annual mission profile. Section IV calculates the time-to-failure of each component, and combines them finally to converter-level reliability. Concluding remarks are drawn in the last section.

II. Reliability Issues in Active Components

A typical configuration of a DFIG is graphically shown in Fig. 2. The partial-scale power converter consists of the Rotor-Side converter (RSC) and the Grid-Side Converter (GSC), due

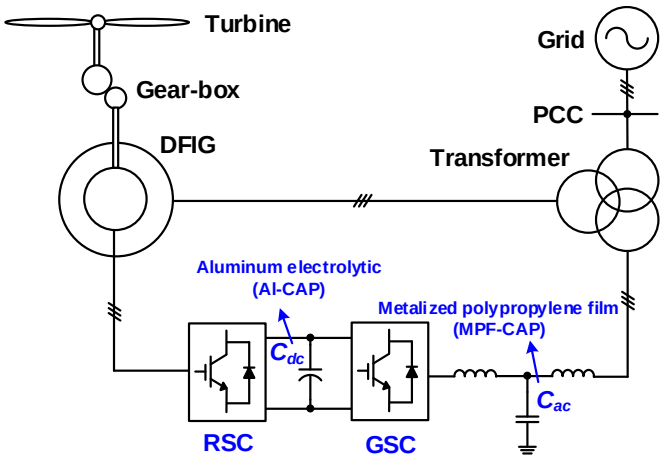

Fig. 2. Typical configuration of a doubly-fed induction generator (DFIG) system. The partial scale power converter consists of the RSC (rotor-side converter) and the GSC (grid-side converter).

to their positions. In between, a DC-link capacitor bank is applied to decouple the back-to-back power converter. Besides, an LCL filter is employed in order to eliminate the high-order harmonics caused by the PWM modulation. As investigated in [2], the power switches and capacitor banks are among the top three fragile components in the power electronic converter, so it is important to evaluate their reliability performance.

To analyze the system, an annual wind speed (Class I) and ambient temperature are shown in Fig. 3(a) and sampled every hour. Since the sample rate is low enough to neglect the dynamics in the turbine and generator, the turbine output power is illustrated in Fig. 3(b). It is worthwhile to note that the cut-in wind speed is 4 m/s, the rated wind speed is 12 m/s, and the cut-off wind speed is 25 m/s.

As the rotor-side active power is the product of the stator-side power and the generator slip, together with the relationship between the slip and wind speed, the power flowing through the back-to-back power converters can be obtained by [19]. The flowchart to estimate the lifetime of the power switches is shown in Fig. 4. With the help of the generator and converter circuit models, the converter voltage

This article has been accepted for publication in a future issue of this journal, but has not been fully edited. Content may change prior to final publication. Citation information: DOI 10.1109/TIA.2020.2977301, IEEE Transactions on Industry Applications

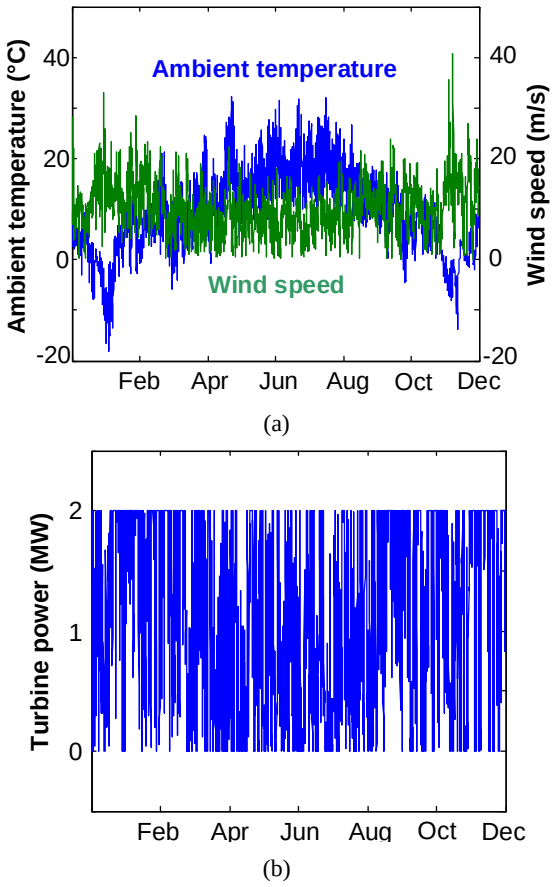

Fig. 3. Annual mission profile of a 2 MW wind turbine with a sample rate of 1 hour. (a) Wind speed and ambient temperature. (b) Turbine output power.

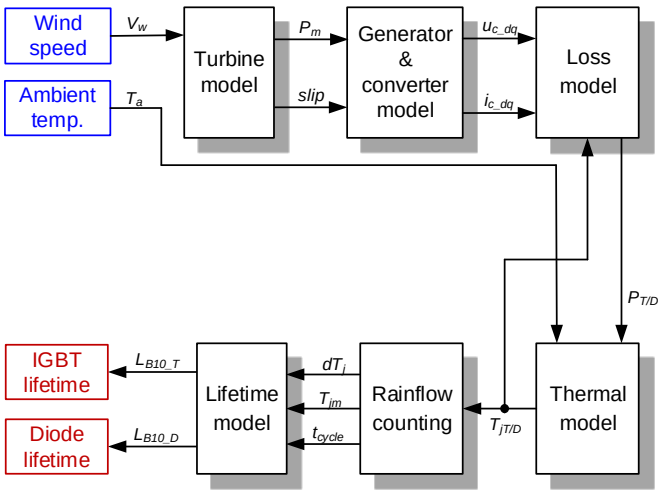

Fig. 4. Flow-chart to calculate B_{10} lifetime of the power switches from mission profile.

and current can be calculated. On the basis of the conduction loss and switching loss, the loss dissipation of the IGBT and the freewheeling diode can be found. By using the thermal model, which only takes into account the thermal resistor of the power device and cooling method (due to the 1-hour sample rate), the junction temperature of the IGBT and the diode can be deduced. As the annual thermal profile is irregular, the Rainflow counting is then applied to extract the thermal cycles with their corresponding amplitude, mean value, and period. The B_{10} lifetime of the IGBT and the diode, which means 10% of the total sample or 10% probability of the component will fail when the operational period reaches the value, can e.g. be calculated according to the Coffin-Manson lifetime model [20]. Detailed mathematical equations of the loss model and thermal model can be found in [19].

A case study is conducted in a 2 MW DFIG system, the specification of which is listed in Table I. The annual

TABLE I
PARAMETERS OF 2 MW DFIG SYSTEM

Rated power	2 MW
Operational range of rotor speed	1050-1800 rpm
Rated amplitude of phase voltage	563 V
Mutual inductance	2.91 mH
Stator leakage inductance	0.04 mH
Rotor leakage inductance	0.06 mH
Ratio of stator winding and rotor winding	0.369
DC-link voltage	1050 V
Grid-side inductor	125 μH
Converter-side inductor	125 μH
DC-link capacitor bank	20 mF
Aluminum electrolytic capacitor	4700 uF/400 V 4 in series & 18 in parallel
AC-side filter capacitor bank	300 μF (Y connection)
Metralized polypropylene film capacitor	10 μF/780 V 10 in parallel (Delta connection)
Switching frequency	2 kHz

TABLE II
PARAMETERS USED IN LOSS MODEL AND THERMAL MODEL OF POWER SEMICONDUCTORS

		IGBT	Diode
Loss model	V_{ce} @ 1 kA, T_j=150 ºC (V)	2.45	/
	V_f @ 1 kA, T_j=150 ºC (V)	/	1.95
	E_{on} @ 1 kA, T_j=150 ºC (mJ)	430	/
	E_{off} @ 1 kA, T_j=150 ºC (mJ)	330	/
	E_{rr} @ 1 kA, T_j=150 ºC (mJ)	/	245
Thermal model	Fourth order thermal resistance R (ºC/kW)	0.3	0.48
		1.6	3.61
		18	34.6
		3.1	6.47
	Fourth order thermal time constant τ (s)	0.003	0.0002
		0.0013	0.0009
		0.04	0.03
		0.4	0.2

This article has been accepted for publication in a future issue of this journal, but has not been fully edited. Content may change prior to final publication. Citation information: DOI 10.1109/TIA.2020.2977301, IEEE Transactions on Industry Applications

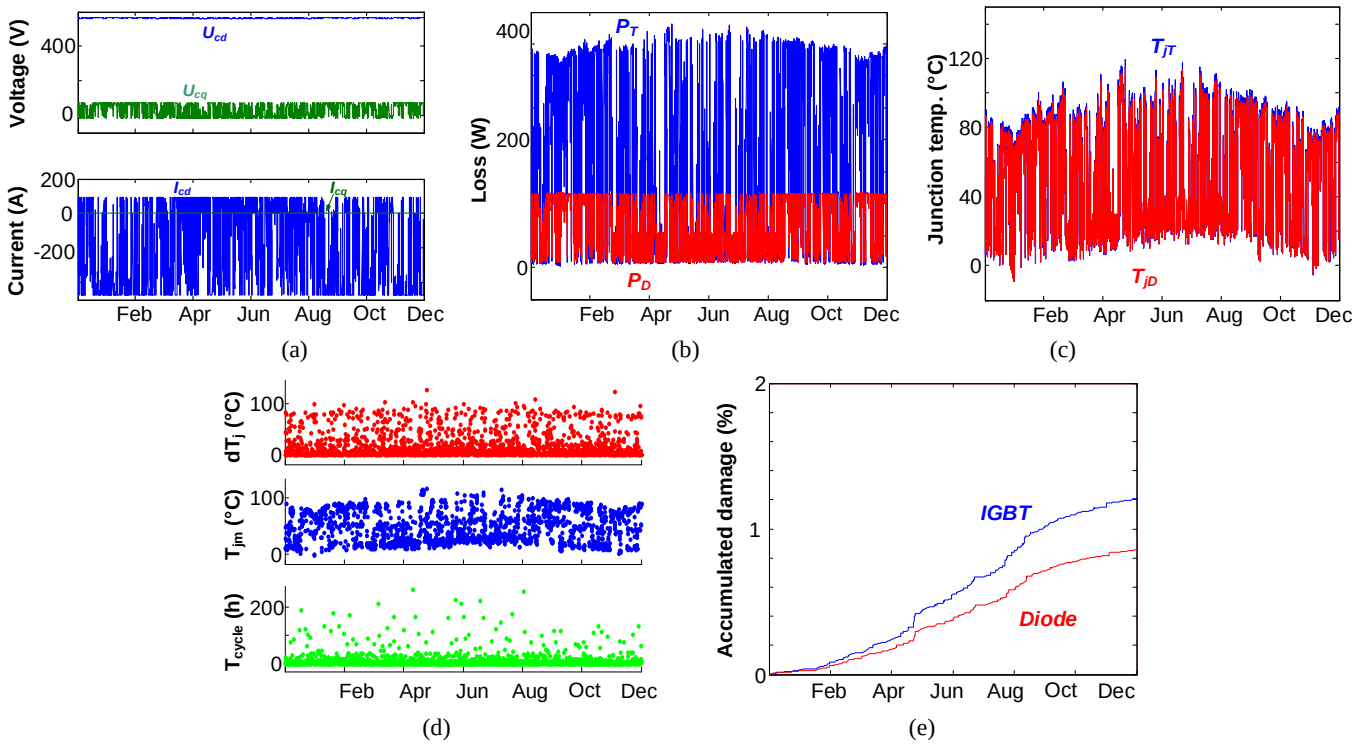

Fig. 5. Annual profile of the IGBT (T) and the diode (D) in the grid-side converter. (a) Electrical stresses. (b) Loss profiles. (c) Thermal profiles. (d) Rainflow counting results. (e) Annual damage.

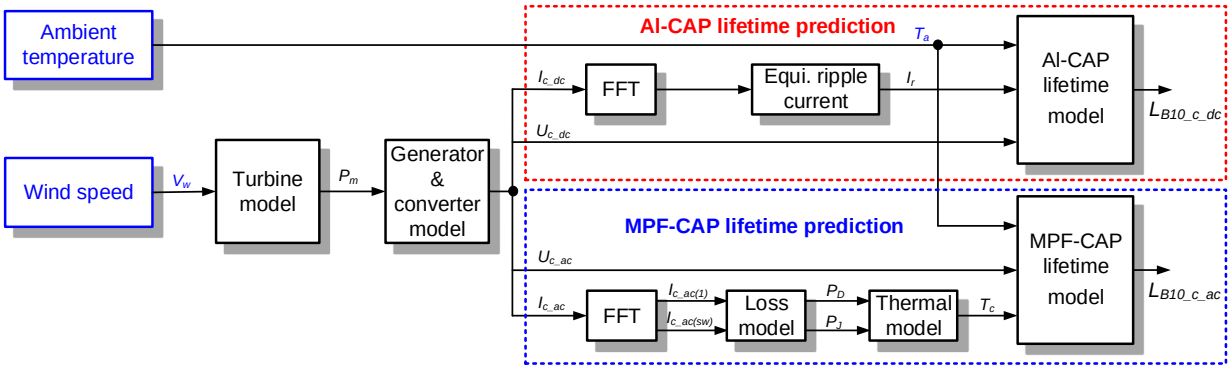

Fig. 6. Flow-chart to calculate B_{10} lifetime of AC-side and DC-link capacitors.

operating profiles of the IGBT and the diode in the GSC are shown in Fig. 5. The key losses and thermal parameters of the power semiconductors are summarized in Table II. As the majority of the power flows from the DC-link to the power grid, it is evident that the IGBT loss is much higher than the diode loss. Nevertheless, the diode chip size is typically almost a half of the IGBT chip, so the junction temperature of the IGBT is just a little higher than the diode. Eventually, it can be seen that the annual damage of the IGBT is 1.2% compared to the diode of 0.9%. Due to the sample rate of 1 hour, it is worthwhile to mention that the minimum period of thermal cycles is higher than 1hours by using Rainflow algorithm. In addition, only the power switches in the GSC is considered.

III. Reliability Issues in Passive Components

In this section, an analytical approach to assess the reliability of power capacitors, both the DC-link capacitor bank (Al-CAP) and AC-side filter capacitor bank (MPF-CAP), is presented considering the annual mission profile. Based on the electrical behavior at various loading conditions, the lifecycle of the single power capacitor can be predicted through its electro-thermal stresses.

According to the mission profile of the wind turbine system, the general procedure to calculate the lifetime of the Al-CAP and MPF-CAP is shown in Fig. 6 [21]. In respect to the Al-CAP, the ripple current can be calculated with the PWM patterns of the power switches in the back-to-back power converters. It is worth mentioning that, considering the

This article has been accepted for publication in a future issue of this journal, but has not been fully edited. Content may change prior to final publication. Citation information: DOI 10.1109/TIA.2020.2977301, IEEE Transactions on Industry Applications

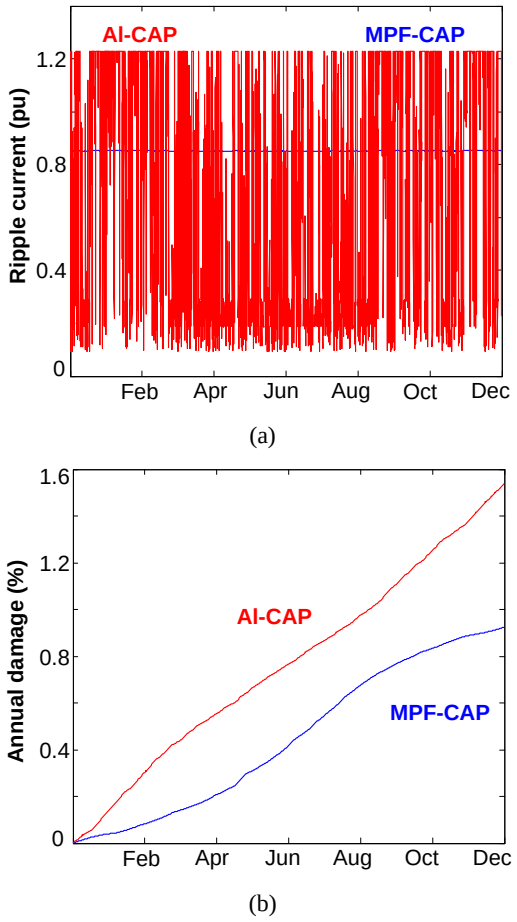

Fig. 7. Annual damage profile comparison between the metalized polypropylene film capacitor (MPF-CAP) and the aluminum electrolytic capacitor (Al-CAP). (a) Ripple current. (b) Accumulated damage.

TABLE III
PARAMETERS OF CAPACITORS THERMAL AND LIFETIME MODELS

	Al-CAP	MPF-CAP
Rated lifetime L_r (hour)	6,000	100,000
Upper categorized temperature T_r (ºC)	105	75
Rated ripple current I_r (A)	13.4	30
Rated voltage V_r (V)	400	780
Core temperature rise at rated ripple current ΔT_o (ºC)	10	/
Coefficient of temperature rise n_1	5	/
Voltage exponent coefficient n_2	5	0.7
ESR (mΩ)	/	3.0
Dissipation factor tanδ	/	2e-4
Thermal resistance from core to ambient (ºC/W)	/	14.1

Equivalent Series Resistor (ESR) curve with various frequencies, the dominating switching harmonics need to be converted to 100 Hz, which is normally specified in the DC-link capacitor datasheet. Together with the ambient temperature profile, the life expectancy of the Al-CAP can be predicted as given in [21].

As the lifetime model of the MPF-CAP is tightly related to its core temperature and the applied voltage, the procedure slightly differs with the Al-CAP. Considering both the dielectric loss and the Joule loss dissipation, the core temperature of the capacitor can be jointly decided by the core-ambient thermal resistance and the ambient temperature profile. With the applied voltage calculated by the PWM pattern of the power switch and the characteristics of the LCL filter, the lifetime of the MPF-CAP can be estimated.

As the sample time interval is much higher than the capacitor thermal time constant (typically several minutes), it can roughly be assumed that the core temperature of the capacitor reaches the steady-state and stays constant within every sample period. The lifetime damage can thereby be calculated by using the sample period over its corresponding hours to failure, which is accumulated from a sample period to the whole operational year.

Based on the key parameters related to the capacitor lifetime prediction listed in Table III, the annual damage of the both types of the capacitors can be deduced and it is shown in Fig. 7, where the lifecycle of the capacitor runs out when the accumulated damage reaches 1. The detailed calculation of ripple current and annual damage for both the Al-CAP and MPF-CAP can be referred to [21]. It is noted that the hours to failure is defined as the B_{10} lifetime. It can be seen that the ripple current of the MPF-CAP is much smoother, as the current harmonic hardly changes with different wind speeds. Moreover, the annual damage of the MPF-CAP is lower, due to the fact that it contains much longer rated lifetime (100,000 hour) compared to the Al-CAP (6,000 hour) under the rated operating condition.

IV. TIME-TO-FAILURE AND RELIABILITY OF POWER CONVERTER

In this section, the percentile lifetime of the single active and passive component will be translated to the Weibull lifetime distribution. Therefore, the converter-level reliability can be linked from the component-level reliability by using a reliability block diagram of the whole system.

In order to fulfill the need of capacitance and be able to withstand the voltage stress, plenty of the capacitors are connected in series or parallel in order to form the capacitor bank. Since any failure of the individual capacitor may result in a degraded performance of the capacitor bank, and any failure of the IGBT or the diode induces the improper operation of the two-level power converter, all of the power switches and capacitors are connected in series in the reliability block diagram as shown in Fig. 8.

Based on the annual damage of both active and passive components shown in Fig. 5(e) and Fig. 7(b), their B_{10} lifetime can be deduced. It is noted that the most stressed IGBT and Al-CAP have the lifetime of 83 and 67 years, respectively.

This article has been accepted for publication in a future issue of this journal, but has not been fully edited. Content may change prior to final publication. Citation information: DOI 10.1109/TIA.2020.2977301, IEEE Transactions on Industry Applications

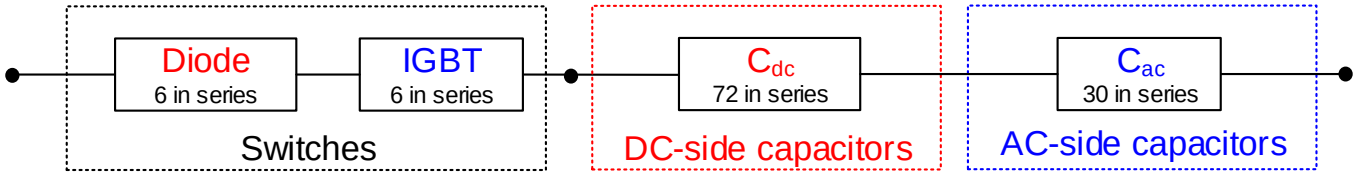

Fig. 8. Converter-level reliability block diagram consisting of the power switches, DC-side capacitors, and AC-side capacitors.

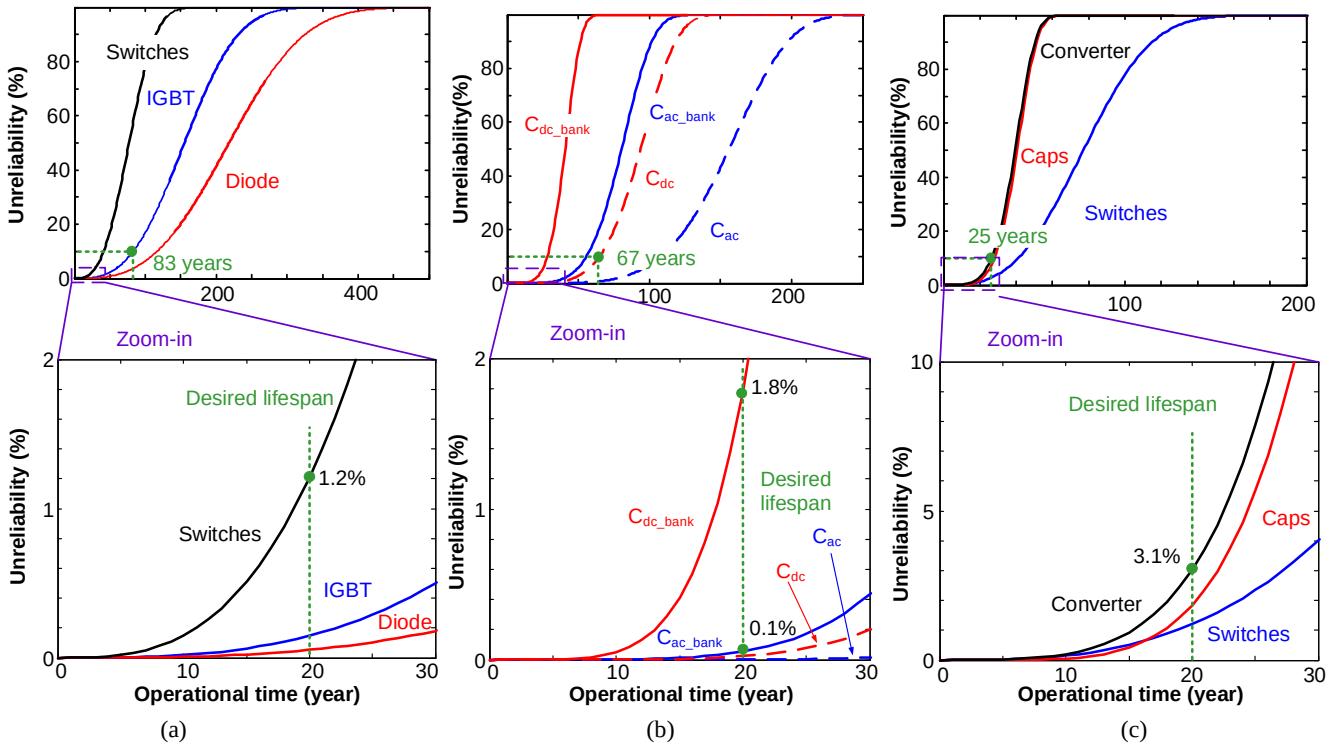

Fig. 9. Unreliability curve from a single component to the whole power converter. (a) From IGBT and diode to power switches (Switches). (b) From single capacitor to capacitor bank (Caps). (c) From switches and capacitors to power converter.

According to [18], the converter-level lifetime is dominated by the most fragile component, which equals to Al-CAP lifetime. However, in order to assess the converter-level reliability accurately, the B_{10} lifetime of the individual component is insufficient, and its time-to-failure distribution, which considers the parameter variations and tolerance uncertainties, is required to apply the reliability block calculation. As the unreliability function $F(t)$ along with the operation period can be expressed by,

$$F(t) = 1 - \exp[-(\frac{t}{\eta})^{\beta}] \quad (1)$$

where β denotes the shape parameter, and η denotes the scaling parameters.

Since the Weibull shape parameters of the power switches and power capacitors are provided in [19], [21], their unreliability curve along with the operational hour can be obtained as shown in Fig. 9(a) and (b). In the case of the series connection in the reliability block diagram, the system-level reliability function is the product of each component reliability. As the sum of the reliability function $R(t)$ and the unreliability/ failure function $F(t)$ is always 1, the following equation exist,

$$F_{sys}(t) = 1 - \prod (1 - F_{com}(t)) \quad (2)$$

where F_{com} is the failure function of the component, and F_{sys} is the failure function of the system.

For the power switches, as the power converter contains six IGBTs and six diodes, at the desired 20-year B_{10} lifetime of the wind power converter, the unreliability value of the total switches significantly increases to 1.2%, while the unreliability value of the individual IGBT is lower than 0.2%. For the power capacitors, it can be seen that the unreliability of the DC-link capacitor bank and the AC-side filter capacitor bank becomes 1.8% and 0.1% at the desired lifespan. The converter-level unreliability is shown in Fig. 9(c), and it is noted that the capacitor bank dominates the converter-level

lifetime. Furthermore, the unreliability value of the desired lifespan is 3.1%, which fulfills the 20-year designed lifecycle. Moreover, if the B_{10} lifetime is considered, it is evident that the converter-level lifetime becomes 25 years, which is much shorter than 67 years estimated by [18]. Furthermore, by using [18], the reliability value at the service life of 20 years cannot be predicted. As a consequence, it can be concluded that the converter-level lifetime is not determined by the most fragile component, as every component has contribution to the system-level reliability. In fact, the system-level lifetime is always shorter than the most fragile component.

V. CONCLUSION

In this paper, the important timescales of the wind turbine system are mapped in terms of the mechanical and electrical parts. In the case of the mission profile with 1-hour sample rate, the circuit model, loss model, and thermal model of the active power switches and passive power capacitors can be considerably simplified. The percentile lifetime of single component can be predicted according to the long-term electro-thermal profile. By considering the parameter variations and component tolerance, the Weibull function based time-to-failure distribution of the active component and passive component can be obtained. In a 2 MW doubly-fed induction generator based wind turbine system, it can be seen that the dc-link capacitor bank dominates the converter-level reliability. This approach serves to better size the critical components to fulfill the total lifecycle design criteria.

References

[1] F. Blaabjerg, and K. Ma, "Future on power electronics for wind turbine systems," *IEEE Journal of Emerging and Selected Topics in Power Electronics*, vol. 1, no. 3, pp. 139-152, Sept. 2013.

[2] H. Wang, M. Liserre, F. Blaabjerg, P. Rimmen, J. Jacobsen, T. Kvisgaard, and J. Landkildehus, "Transitioning to physics-of-failure as a reliability driver in power electronics," *IEEE Journal of Emerging and Selected Topics in Power Electronics*, vol. 2, no. 1, pp. 97-114, Mar. 2014.

[3] L. M. Moore, and H. N. Post, "Five years of operating experience at a large utility-scale photovoltaic generating plant," *in Prog. Photovolt.: Res. Appl.*, vol. 16, no. 3, pp. 249-259, 2008.

[4] S. Yang, A. Bryant, P. Mawby, D. Xiang, L. Ran, and P. Tavner, "An industry-based survey of reliability in power electronic converters," *IEEE Trans. on Industry Applications*, vol. 47, no. 3, pp. 1441-1451, Jun. 2011.

[5] ABB Application Note, *Load-cycling capability of HiPak IGBT modules*, 2012.

[6] G. Zhang, D. Zhou, J. Yang, and F. Blaabjerg. "Fundamental-frequency and load-varying thermal cycles effects on lifetime estimation of DFIG power converter," *Microelectronics Reliability*, vol. 76, pp. 549-555, 2017.

[7] D. Zhou, F. Blaabjerg, M. Lau, and M. Tonnes, "Thermal behavior optimization in multi-MW wind power converter by reactive power circulation," *IEEE Trans. on Industry Applications*, vol. 50, no. 1, pp. 433-440, Jan. 2014.

[8] D. Zhou, and F. Blaabjerg, "Converter-level reliability of wind turbine with low sample rate mission profile," *in Proc. of IEEE ICPE 2019 - ECCE Asia*, pp. 3309-3314, 2019.

[9] H. Jedtberg, M. Langwasser, R. Zhu, G. Buticchi, and M. Liserre, "Impacts of rotor current control targets on DC-link capacitor lifetime in DFIG-based wind turbine during grid voltage unbalance," *in Proc. of IEEE ECCE 2017*, pp. 3489-3495, 2017.

[10] B. P. McGrath, and D. G. Holmes, "A general analytical method for calculating inverter DC-link current harmonics," *IEEE Trans. on Industry Applications*, vol. 45, no. 5, pp. 1851-1859, Sept. 2009.

[11] X. Pei, W. Zhou, and Y. Kang, "Analysis and calculation of DC-link current and voltage ripples for three-phase inverter with unbalanced load," *IEEE Trans. on Power Electronics*, vol. 30, no. 10, pp. 5401-5412, Oct. 2015.

[12] C. Liu, D. Xu, N. Zhu, F. Blaabjerg, and M. Chen, "DC-voltage fluctuation elimination through a DC-capacitor current control for DFIG converters under unbalanced grid voltage conditions," *IEEE Trans. on Power Electronics*, vol. 28, no. 7, pp. 3206-3218, July 2013.

[13] M. H. Bierhoff, and F. W. Fuchs, "DC-link harmonics of three-phase voltage-source converters influenced by the pulse width-modulation strategy—an analysis," *IEEE Trans. on Industrial Electronics*, vol. 55, no. 5, pp. 2085-2092, May 2008.

[14] M. Liserre, R. Teodorescu, and F. Blaabjerg, "Stability of photovoltaic and wind turbine grid-connected inverters for a large set of grid impedance values," *IEEE Trans. on Power Electronics*, vol. 21, no. 1, pp. 263-272, Jan. 2006.

[15] G. Shen, X. Zhu, J. Zhang, and D. Xu, "A new feedback method for PR current control of LCL-filter-based grid-connected inverter," *IEEE Trans. on Industrial Electronics*, vol. 57, no. 6, pp. 2033-2041, June 2010.

[16] D. Zhou, F. Blaabjerg, M. Lau, and M. Tonnes, "Optimized reactive power flow of DFIG power converters for better reliability performance considering grid codes," *IEEE Trans. on Industrial Electronics*, vol. 62, no. 3, pp. 1552-1562, Mar. 2015.

[17] K. Ma, M. Liserre, F. Blaabjerg, and T. Kerekes, "Thermal loading and lifetime estimation for power device considering mission profiles in wind power converter," *IEEE Trans. on Power Electronics*, vol. 30, no. 2, pp. 590-602, Feb. 2015.

[18] H. Liu, K. Ma, Z. Qin, P. C. Loh, and F. Blaabjerg, "Lifetime estimation of MMC for offshore wind power HVDC application," *IEEE Journal of Emerging and Selected Topics in Power Electronics*, vol. 4, no. 2, pp. 504-511, June 2016.

[19] D. Zhou, G. Zhang, and F. Blaabjerg, "Optimal selection of power converter in DFIG wind turbine with enhanced system-level reliability," *IEEE Tran. on Industry Applications*, vol. 54, no. 4, pp. 3637-3644, Jul. 2018.

[20] P. Lall, M. N. Islam, M. K. Rahim, and J. C. Suhling, "Prognostics and health management of electronic packaging," *IEEE Trans. on Components and Packaging Technologies*, vol. 29, no. 3, pp. 666-677, Sep. 2006.

[21] D. Zhou, Y. Song, Y. Liu, and F. Blaabjerg, "Mission profile based reliability evaluation of capacitor banks in wind power converters," *IEEE Trans. on Power Electronics*, vol. 34, no. 5, pp. 4665-4677, May 2019.